Supplementary Materials

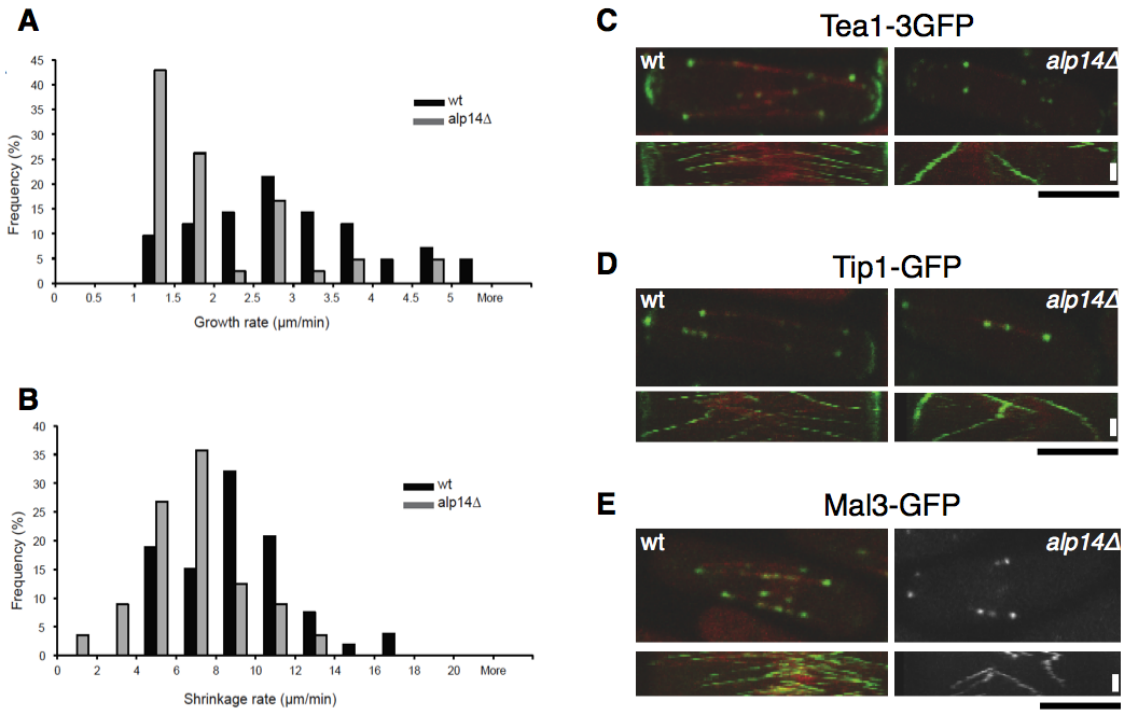

Supplementary Figure 1. Microtubule dynamics in *alp14*Δ mutant cells.

A, B) Measurements of MT growth and shrinkage rates in vivo. Histograms show the distribution of rates measured from interphase MTs in wildtype (FC1234) and *alp14*Δ (FC2332) mutant cells.

C, D) Localization of Tea1-GFP (a cell polarity protein) and Tip1-GFP (CLIP-170) in *alp14*Δ cells expressing mRFP-tubulin (FC2469 and FC2470 respectively). Images and kymographs are shown. The plus end localization patterns of these +TIP proteins are not perturbed in *alp14*Δ mutant cells. Scale bar = 5um. Time scale bar = 30sec.

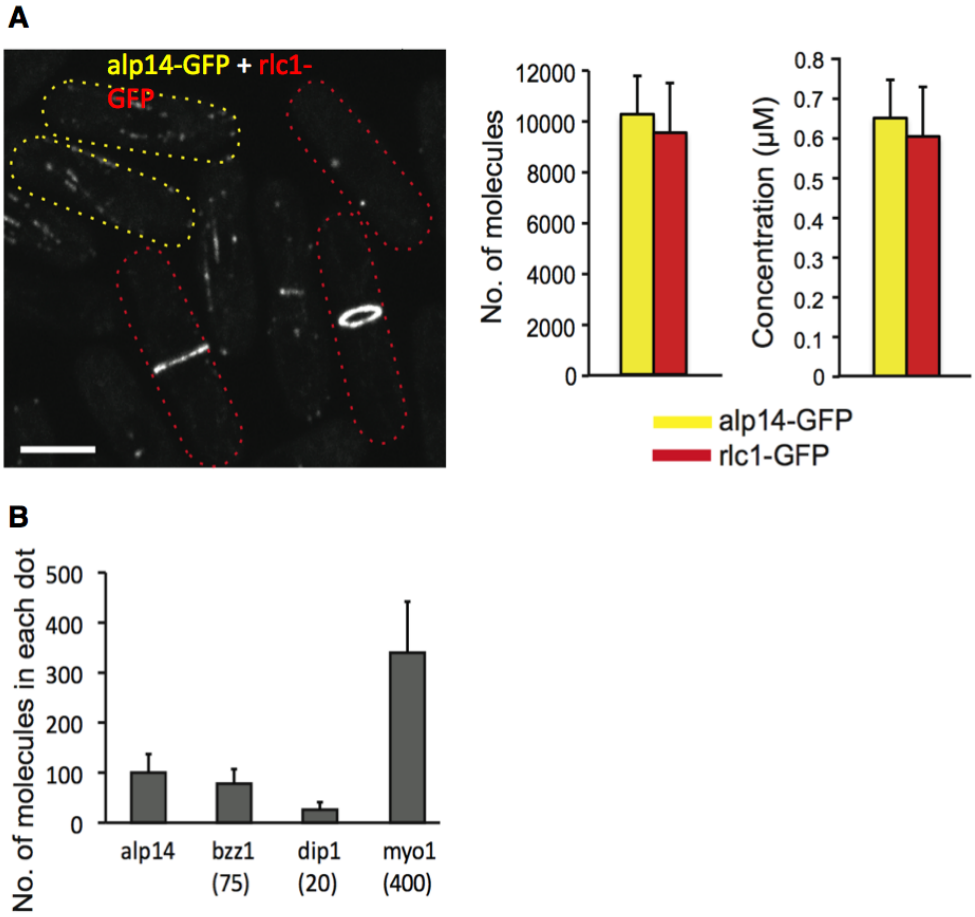

Figure S2. Counting Alp14 molecules.

Cells expressing Alp14-GFP were mixed with cells expressing other GFP fusion proteins and imaged in the same microscope field. The different localization patterns made it possible to distinguish the Alp14-GFP cells from the other cells. Fluorescence intensity measurements were taken and compared with proteins that had been quantitated previously (Wu and Pollard, 2005; Basu and Chang, 2011; Sirotkin *et al*., 2011).

(A) Comparison of Alp14-GFP and Rlc1-GFP (myosin light chain) cells provides an estimate of Alp14-GFP total concentration in the cell. (n=13 cells for Alp14-GFP; n=15 for Rlc1-GFP).

(B) Comparison with endocytic patch proteins such as Bzz1, which form small dots like Alp14, provide an estimate of the number of Alp14 molecules at a single MT plus end. Values in parentheses represent published numbers. These data have been scaled to Buzz1 as 75 molecules/dot. Strains are FC1907 Alp14-GFP, FC1139 Rlc1-GFP, FC2033 Cnp1-GFP, FC1153 Myo1-GFP, FC2588 Dip1-GFP.

Protein	Calculated Mass	Elution Volume	Stokes Radius	Apparent Weight	Measured Mass
αβ-tubulin	101 kDa	14.01 mL	~41 Å	85 kDa	N/A*
Alp14 (dimer)	200 kDa	9.70 mL	~33 Å	550 kDa	198± 5 kDa
Alp14: tubulin	301 kDa	9.50 mL	~37 Å	630 kDa	301±10kDa
Alp14-GFP	240 kDa	9.60 mL	~45 Å	600 kDa	N/A*

Alp14 Mass and Hydrodynamic Properties

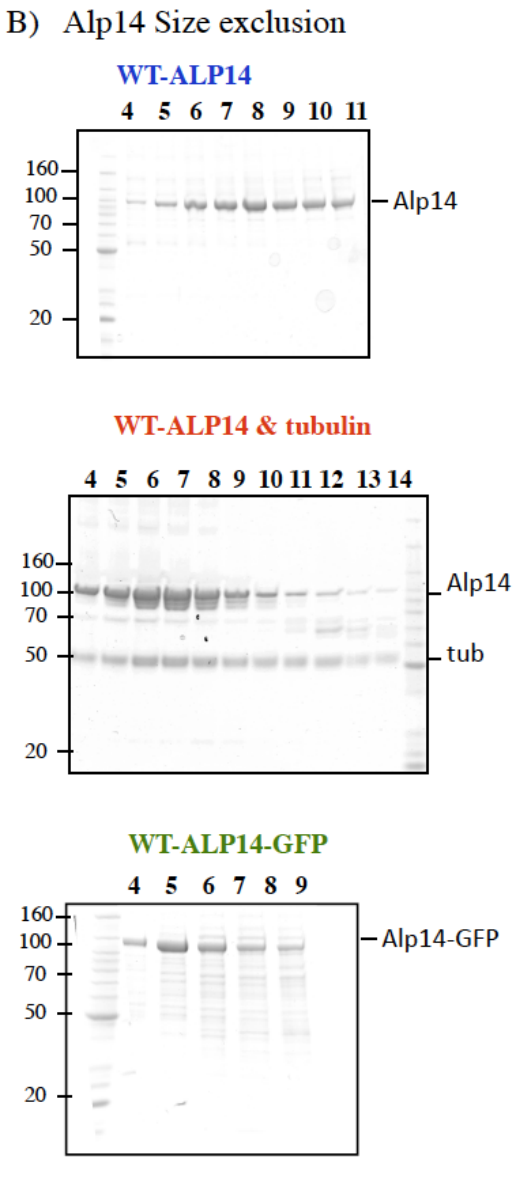

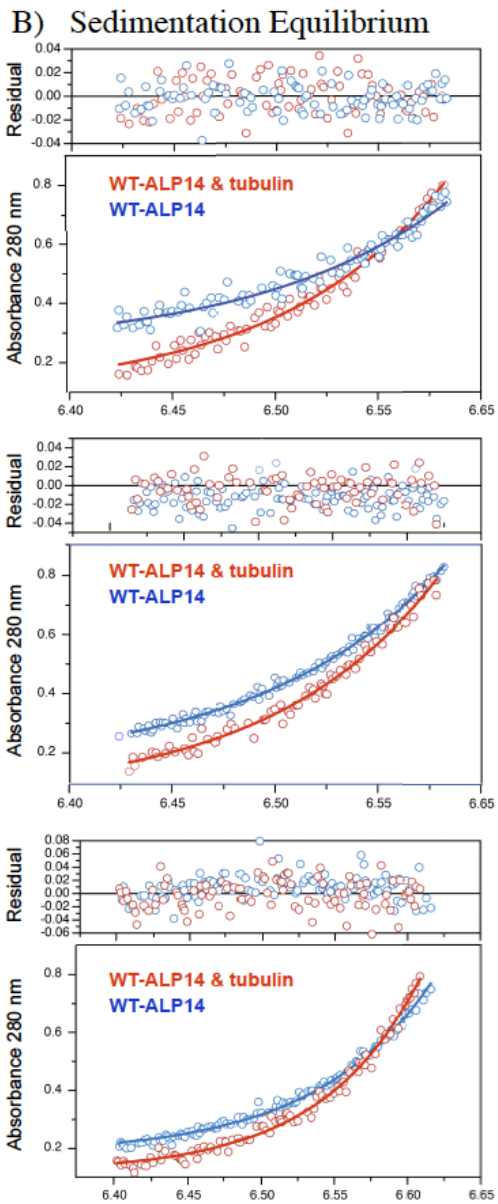

Supplementary Figure S3: The hydrodynamic and mass parameters for Alp14 and Alp14-tubulin complexes

A) Table describing masses and apparent molecular weights of tubulin, Alp14, Alp14-Tubulin and Alp14-GFP that are measured with size exclusion chromatography or sedimentation equilibrium ultracentrifugation. * marks proteins or complexes were not measured or were not stable enough for measuring mass by sedimentation equilibrium analytical ultracentrifugation. † marks the mass differences between Alp14: tubulin and Alp14 to be ~100 kDa, indicating a stoichiometry of 1 tubulin dimer per Alp14 dimer. B) Size exclusion profiles of Wt-Alp14 (blue), Wt Alp14- tubulin complex (red), Alp14-GFP (green). C) Sedimentation equilibrium analytical ultracentrifugation of Alp14 and purified Alp14-tubulin complexes at 3500 g, 5000 g and 8300 g. The lower panels show raw data (Alp14: blue points, Alp14p-tubulin: red points) and calculated fit (Alp14 blue lines, Alp14-tubulin: red lines) at the masses reported in the table A. The upper panels show the residual differences between actual data and the calculated fitted lines.

Supplementary Table S1: Parameters of dynamic microtubules with Alp14 measured by TIRF microscopy

Condition	Assembly N	Assembly Rate	Assembly Period	Disassembly N	Disassembly Rate	Disassembly Period	Catastrophe N	Catastrophe Frequency	MT length N	MT length
6 μM tubulin	98	0.41 ± 0.07	361 ± 164	81	35.2 ± 0.4	4.5 ± 1.7	56	0.17 ± 0.08	82	2.38 ± 0.1
20 nM Alp14	106	0.70 ± 0.02*	354 ± 156	87	36.6 ± 1.1	4.6 ± 2.2	84	0.19 ±0.08	103	3.54 ± 0.2
40 nM Alp14	35	0.92 ± 0.01**	286 ± 107	34	42.0 ± 0.9*	6.5 ± 3.5	28	0.19 ± 0.07	33	5.05 ± 0.2
60 nM Alp14	74	1.09 ± 0.02**	324 ± 178	58	44.7 ± 1.1*	8.1 ± 4.6	40	0.18 ± 0.08	93	5.60 ± 0.3
100 nM Alp14	34	1.33 ± 0.03**	297 ± 138	25	43.2 ± 8.4*	8.3 ± 3.8	26	0.22 ±0.07	25	6.14 ± 0.4
200 nM Alp14	40	0.91 ± 0.03**	289 ±128	50	45.5 ± 2.1*	6.4 ± 2.7	25	0.21 ± 0.07	25	4.45 ± 0.4
300 nM Alp14	80	0.49 ± 0.01	277 ± 145	45	42.9 ± 1.0	3.3 ± 1.4	40	0.23 ± 0.07	80	2.53 ± 0.1
1000 nM Alp14	50	0.35 ± 0.01	155 ± 68	60	48.7 ± 2.75	2.2 ± 1.3	25	0.26 ± 0.10†	60	0.68 ± 0.1
							20	0.50 ± 0.07†		
25 nM Alp14-GFP	32	0.79 ± 0.03	251 ± 103	32	38.2 ± 1.18	6.8 ± 3.4	32	0.22 ±0.02	32	4.98 ±0.7
+ Alp14 GFP ends	14	0.91 ± 0.02	220 ± 107	14	36.9 ± 2.1	6.8 ± 3.7	14	0.23 ± 0.01	14	3.61 ±0.7
- Alp14 GFP ends	18	0.66 ± 0.02	281 ± 93	18	38.3 ± 1.4	6.9 ± 3.3	18	0.22 ± 0.04	18	4.37 ± 0.3
20 nM Alp14 ^{T1T3}	40	0.37 ± 0.01	176 ± 106	23	35.6 ± 3.3	3.3 ± 3.0	40	0.25 ± 0.02	40	2.07 ± 0.1
40 nM Alp14 ^{T1T3}	33	0.38 ± 0.02	231 ± 81	23	36.0 ± 1.0	4.5 ± 1.8	25	0.21 ± 0.03	33	2.23 ± 0.1
60 nM Alp14 ^{T1T3}	75	0.32 ± 0.02	238 ± 154	70	32.0 ± 1.4	4.6 ± 2.9	65	0.21 ± 0.09	75	1.62 ± 0.1
100 nM Alp14 ^{T1T3}	40	0.30 ± 0.09	210 ± 50	25	31.5 ± 16	4.4 ± 2.1	28	0.23 ± 0.06	33	1.55 ± 0.2

Units: Assembly rate (μm/min), Assembly period (sec), Disassembly rate (μm/min) Disassembly period (sec),
Catastrophe Frequency (min^{-1}) Rescue Frequency (min^{-1}), MT length (μm)

Error reported is Standard Error Mean (SEM).

*Conditions significantly differ from 6 μM tubulin control at p> 0.1
** Conditions differ significantly from the 6 μM tubulin control at p> 0.001

For Assembly and disassembly rates, N is the number of assembly and disassembly events
For Catastrophe, N is the number of microtubules observed.
† these data showed a bimodal distribution and were fit with two Gaussian curves resulting into two different average rates.

Supplementary Table S2: MT assembly rates at different soluble tubulin and Alp14 concentrations.

	6 μM tubulin	**8 μM tubulin**	**10 μM tubulin**
0 nM Alp14	0.509 ± 0.014	0.841 ± 0.015	0.987 ± 0.025
200 nM Alp14	0.956 ± 0.014	1.365 ± 0.016	1.485 ± 0.039
250 nM Alp14	No MT assembly	0.976 ± .0028	1.230 ± 0.025
300 nM Alp14	No MT assembly	0.962 ± 0.034	1.189 ± 0.031
500 nM Alp14	No MT assembly	No MT assembly	0.943 ± 0.019

Microtubule assembly rates (μm/min) were measured for five different Alp14 concentrations, each with three different tubulin dimer concentrations using TIRF microscopy. The values reported here support the bar graph presented in Figure 3H.

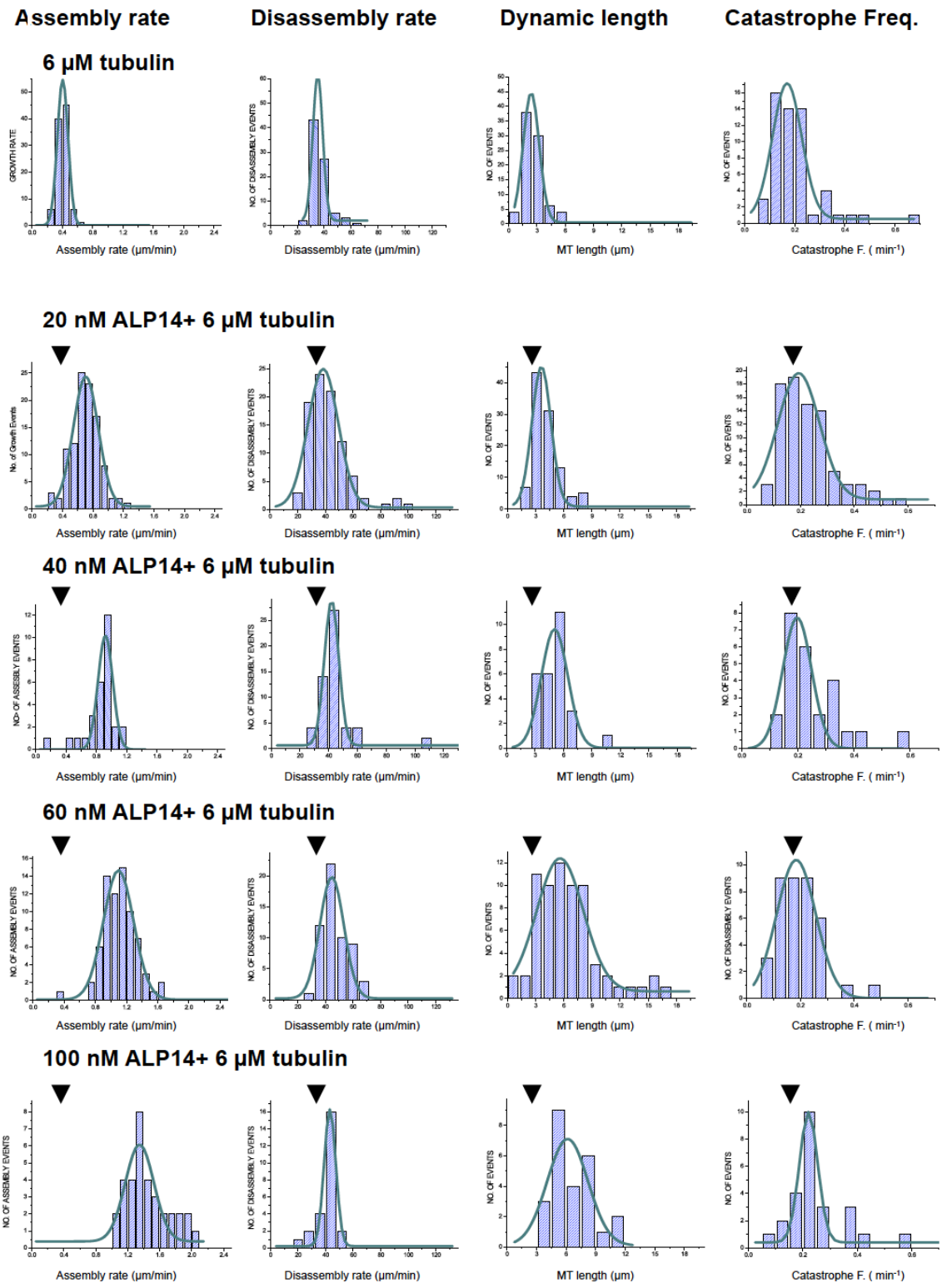
Assembly rate
Disassembly rate
Dynamic length
Catastrophe Freq.
6 µM tubulin
20 nM ALP14+ 6 µM tubulin
40 nM ALP14+ 6 µM tubulin
60 nM ALP14+ 6 µM tubulin
100 nM ALP14+ 6 µM tubulin
GROWTH RATE
NO. OF DISASSEMBLY EVENTS
NO. OF EVENTS
No. of Growth Events
NO. OF ASSEMBLY EVENTS
Assembly rate (µm/min)
Disassembly rate (µm/min)
MT length (µm)
Catastrophe F. (min-1)

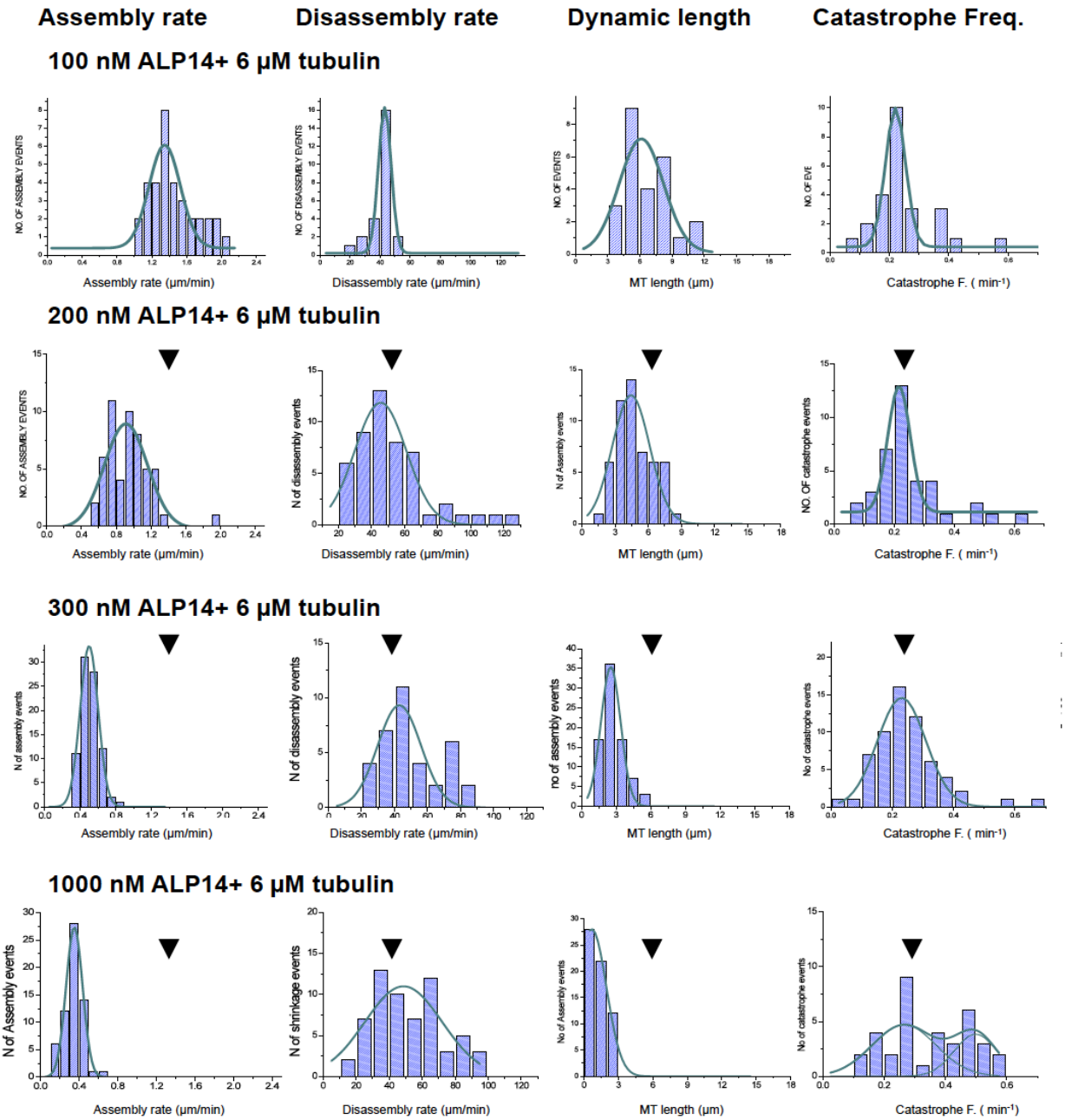

Supplementary Figure S4: A) The distributions of raw MT dynamic parameters with 0-1000 nM Alp14.

The distributions of MT dynamic parameter were measured from a large number of kymographs for (shown in Fig 4) of dynamic TIRF experiment and the values were pooled for each experimental condition. The distributions of each parameter are plotted as the frequency of each event per number of observed events in each experiment.

Distributions shown for the conditions as listed. Fitted Gaussians were used to fit the data and to estimate the average value of each parameter. Black arrows mark the peak averages of MT dynamics parameters in 6 μM tubulin dimer to compare with other conditions. Black arrows on each curve mark the peak averages of MT dynamics parameters at maximum MT polymerase at 100 nM Alp14+6 μM tubulin dimer.

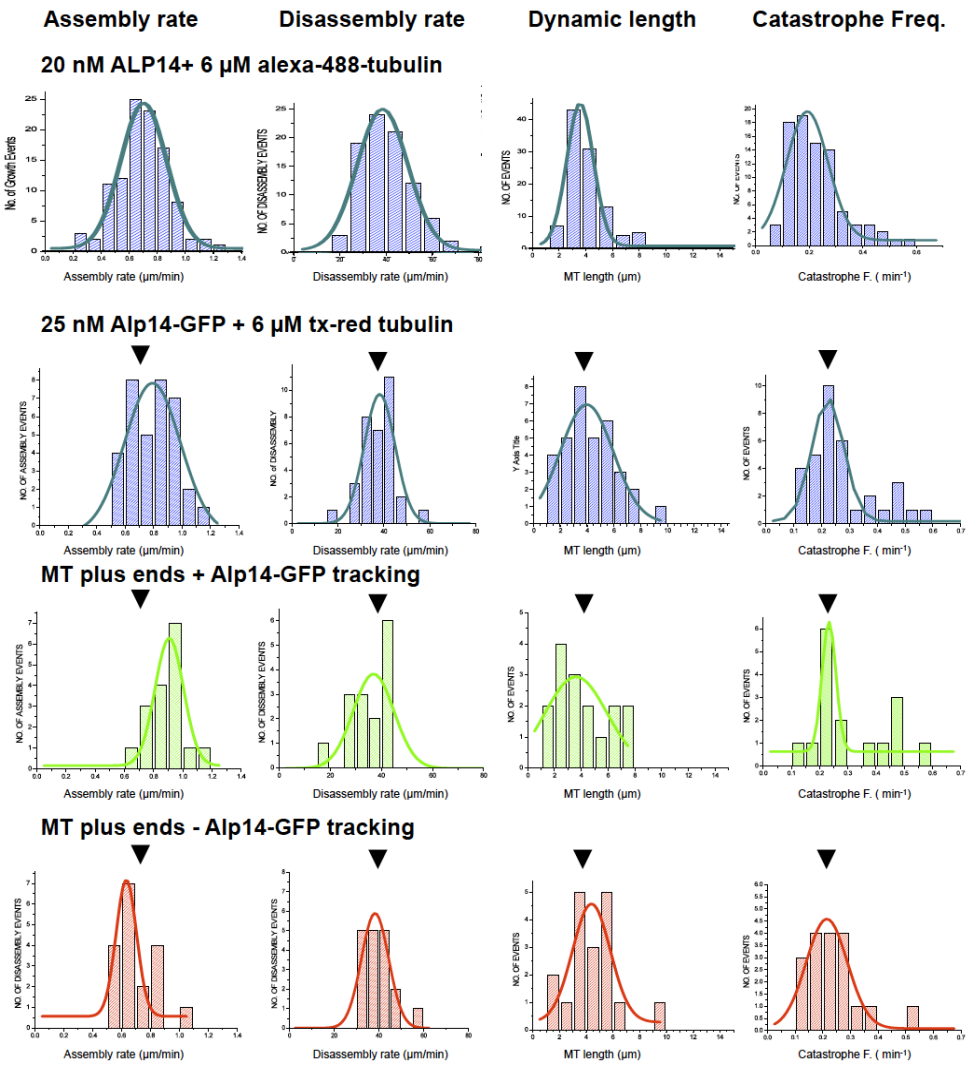

Supplementary Figure S5: A) Distributions of MT measurements.

The distributions of MT dynamic parameter were measured from kymographs (shown in Fig 4) of a dynamic TIRF experiment with 25 nM Alp14+ 6 µM tubulin dimer. The total MT dynamic parameters (blue curves) are compared to dynamic parameters of MT ends with Alp14-GFP plus tracking (green curves) and those of dynamic MTs ends where Alp14-GFP tracking was not observed (red curves). Data from each group was pooled and the distributions of each parameter are plotted as the frequency of each event per number of observed events in each experiment. Black arrows on each curve mark the peak averages of MT dynamics parameters of the average 25 nM Alp14 + 6 µM tubulin total data. Note the Alp14-GFP tracking MT assembly rate events (green curve) have a

two fold higher MT assembly rate on average compared to the average MT assembly rate without Alp14 plus end tracking (red curve).

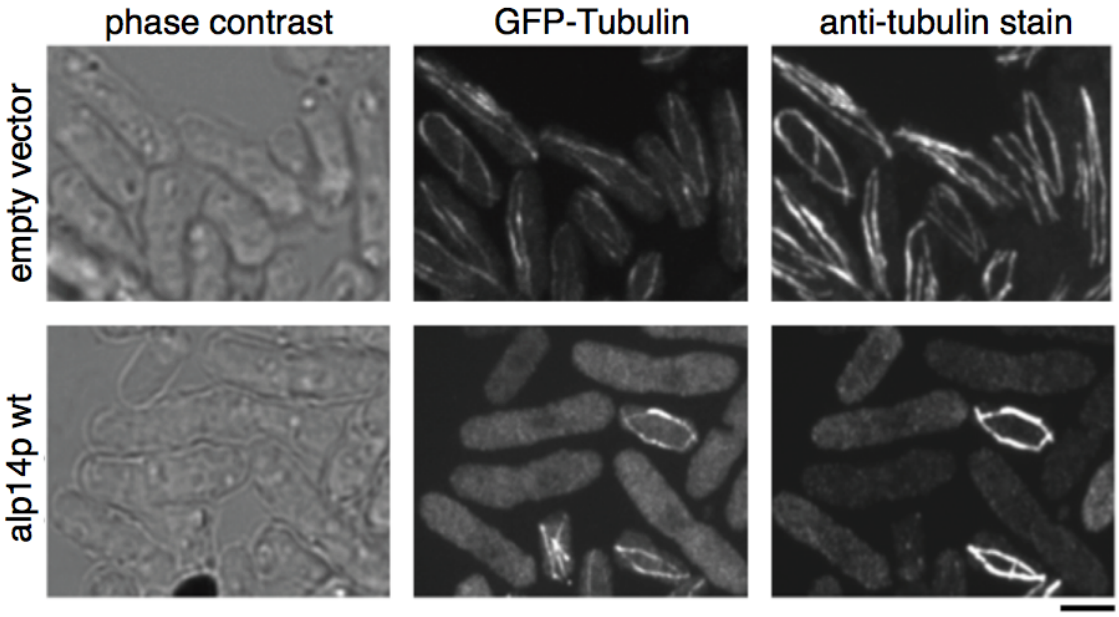

Supplementary Figure S6. Alp14 overexpression leads to loss of MTs.

GFP-tubulin cells overexpressing alp14 (FC2477) (as described in text) were fixed and stained for MTs using anti-tubulin antibody. Note that most of the alp14 overexpressing cells lack MTs, as shown by both GFP-tubulin and anti-tubulin staining. The small percentage of cells that exhibit MTs likely express lower levels of alp14p.

For MT staining (Marks *et al.*, 1986), cells were fixed with cold methanol, permeabilized in 1% Triton X-100 in PEMS (100 mM PIPES, pH 6.9, 1 mM EGTA, 1 mM $MgSO_4$, 1 M Sorbitol) then incubated with 1/100 TAT antibody (from Keith Gull) as 1˚ antibody and 1/500 dilution of Alexa Fluor 594 goat anti-mouse IgG (Invitrogen, A-11032) as 2˚ antibody in PEMBAL (PEM, 1% BSA).

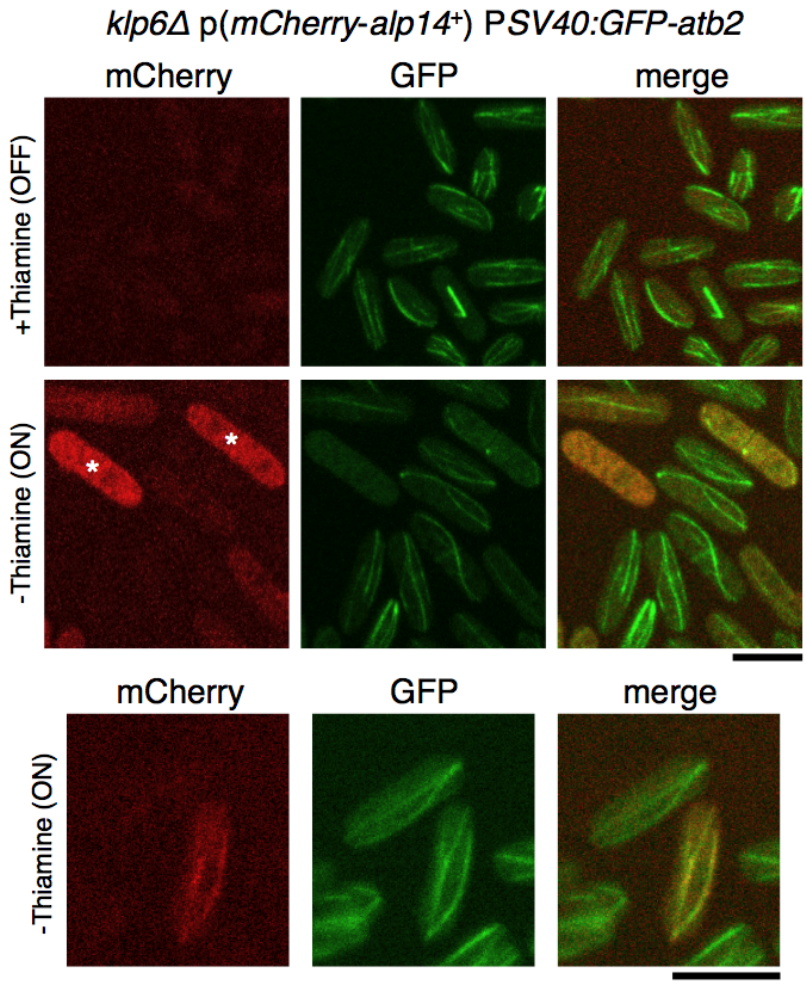

Supplementary Figure S7. The loss of MTs seen with overexpression of Alp14 is independent of the depolymerase Klp6.

An *nmt1-mCherry-Alp14* plasmid was introduced into a *klp6*Δ mutant strain (FC2648) and grown in media with thiamine (repressive conditions) or absence of thiamine (inducing conditions) for 16 hours at 25˚C. Alp14 and GFP-tubulin were imaged, with maximum intensity projection images shown. Astericks label cells overexpressing Alp14, which have largely lost MTs. Bottom set of images show a cell at moderate level of expression, in which MTs are still intact and Alp14p is seen along the MT lattice. Scale bar = 10um.

Supplementary Table 3: *S. pombe* strains used in this study

Strain	Genotype	Source/Reference
FC1234	*h- leu1-32::pSV40-GFP-atb2(leu1+) ade6- leu1-32 ura4-D18*	Chang Lab
FC1907	*h- alp14-GFP-kan leu1- ura4- his7-*	Chang Lab
FC2332	*h+ alp14::ura4+ leu1-32::SV40-GFP-atb2[LEU1] ade6? leu1- ura4-*	This study
FC2336	*h? tip1-GFP:kanMX alp14-rRFP-kan ade6? leu1- ura4-*	Chang Lab
FC2347	*h? mal3-GFP:kanMX alp14-rRFP-kan ade6? leu1- ura4-*	Chang Lab
FC2470	*h? tip1:GFP-KanMX alp14::ura4+ ade6? leu1- ura4- [pSB62[nmt41-mRFP-tub1;LEU2]]*	This study
FC2471	*h? tea2::his3+ alp14-GFP-KanMX ade6? leu1- ura4- his7+ [pSB62[nmt41-mRFP-tub1;LEU2]]*	This study
FC2472	*h+ mal3::NatMX alp14-GFP-KanMX ade6? leu1- ura4- his7+ [pSB62[nmt41-mRFP-tub1;LEU2]]*	This study
FC2476	*h- leu1-32::SV40-GFP-atb2[LEU1+] leu1- ura4- [pSB67[nmt41-mCherry;URA4+]]*	This study
FC2477	*h- alp14::NatMX leu1-32::SV40-GFP-atb2[LEU1+] leu1- ura4- [pHK10[nmt41-mCherry-alp14;URA4+]]*	This study
FC2478	*h- leu1-32::SV40-GFP-atb2[LEU1+] leu1- ura4- [pHK11[nmt41-mCherry-alp14 MT9(W23A R109A W300A K381A);URA4+]]*	This study
FC2479	*h- leu1-32::SV40-GFP-atb2[LEU1+] leu1- ura4- [pHK12[nmt41-mCherry-alp14 TOG (1-509 aa);URA4+]]*	This study
FC2480	*h- leu1-32::SV40-GFP-atb2[LEU1+] leu1- ura4- [pHK14[nmt41-mCherry-alp14 MT5(W23A R109A);URA4+]]*	This study
FC2481	*h- leu1-32::SV40-GFP-atb2[LEU1+] leu1- ura4- [pHK15[nmt41-mCherry-alp14 MT6(W300A K381A;URA4+]]*	This study
FC2482	*h- leu1-32::SV40-GFP-atb2[LEU1+] ade6- leu1- ura4- [pHK16[nmt41-mCherry-alp14 Cterm;URA4+]]*	This study
FC2483	*h+ alp14::NatMX leu1-32::SV40-GFP-atb2[LEU1+] leu1- ura4- [pSB67[nmt41-mCherry;URA4+]]*	This study
FC2484	*h+ alp14::NatMX leu1-32::SV40-GFP-atb2[LEU1+] leu1- ura4- [pHK10[nmt41-mCherry-alp14;URA4+]]*	This study
FC2485	*h+ alp14::NatMX leu1-32::SV40-GFP-atb2[LEU1+] leu1- ura4- [pHK11[nmt41-mCherry-alp14 MT9(W23A R109A W300A K381A);URA4+]]*	This study
FC2486	*h- alp14::NatMX leu1-32::SV40-GFP-atb2[LEU1+] leu1- ura4- [pHK12[nmt41-mCherry-alp14 TOG (1-509 aa);URA4+]]*	This study
FC2487	*h+ alp14::NatMX leu1-32::SV40-GFP-atb2[LEU1+] leu1- ura4- [pHK14[nmt41-mCherry-alp14 MT5(W23A R109A);URA4+]]*	This study
FC2488	*h+ alp14::NatMX leu1-32::SV40-GFP-atb2[LEU1+] leu1- ura4- [pHK15[nmt41-mCherry-alp14 MT6(W300A K381A;URA4+]]*	This study

FC2489	*h+ alp14::NatMX leu1-32::SV40-GFP-atb2[LEU1+] leu1-ura4- [pHK16[nmt41-mCherry-alp14 Cterm;URA4+]]*	This study
FC2493	*h- alp14-GFP-KanMX ade6? leu1- ura4- his7- [pSB62[nmt41-mRFP-tub1;LEU2]]*	This study
FC2494	*h- alp14-GFP-KanMX tip1::KanMX ade6? leu1- ura4- his7- [pSB62[nmt41-mRFP-tub1;LEU2]]*	This study
FC2648	*h- klp6::his ade6- leu1-32 ura4-D18 his7- [pHK10[nmt41-mCherry-alp14;URA4+]]*	This study

Supplemental Table 4: Oligonucleotides used in this study

Name	Sequence (5'→3')
oHK24	AGTCCCGGGGTGAATCAATCCCTGATGTCT
oHK35	GTACATAAAGTAGCGAAAGTGCGTCTATCTGC
oHK36	GCAGATAGACGCACTTTCGCTACTTTATGTAC
oHK37	GCTTAACATCACCTGCCGCAGGTACAAGG
oHK38	CCTTGTACCTGCGGCAGGTGATGTTAAGC
oHK39	GGCTTCTTCGAAAGCGAAGGATCGTAAGG
oHK40	CCTTACGATCCTTCGCTTTCGAAGAAGCC
oHK41	CGATCCAAAGAGAAAGCGGCTAATGTAATCG
oHK42	CGATTACATTAGCCGCTTTCTCTTTGGATCG
oHK49	AGTCCCGGGTGCCTTAGCCTTTACTGTAGCTGT
oHK55	AGTGTCGACATGAGCCAAGATCAAGAAGAA
oHK57	AGTCCCGGGATGAGCCAAGATCAAGAAGAAGAC

Supplemental Table 5: Plasmids used in this study

Name	Description	Selection Markers
pSB62	pREP41X-mRFP-tub1	amp *LEU2*
pSB67	pREP41X-*mCherry*	amp *ura4*$^+$
pHK10	pREP41X-*mCherry-alp14*	amp *ura4*$^+$
pHK11	pREP41X-*mCherry*-alp14 TOG1,2$^-$ MT9(W23A R109A W300A K381A)	amp *ura4*$^+$
pHK12	pREP41X-*mCherry*-alp14 TOG (1-509 aa)	amp *ura4*$^+$
pHK14	pREP41X-*mCherry*-alp14 TOG1$^-$ MT5(W23A R109A)	amp *ura4*$^+$
pHK15	pREP41X-*mCherry*-alp14 TOG2$^-$ MT6(W300A K381A)	amp *ura4*$^+$
pHK16	pREP41X-*mCherry*-alp14Cterm(510-809aa)	amp *ura4*$^+$

Supplementary Movie Legends

Movie 1. Alp14 tracks growing MT plus ends in fission yeast. Time-lapse images of interphase cells expressing Alp14-GFP (green) and RFP-tubulin (red). Total time =3 min (4 sec/frame). Strain is FC2493.

Movie 2. Alp14 tracks growing MT plus ends in the absence of Mal3 (EB1). Time lapse images of a *mal3*Δ cell expressing Alp14-GFP (green) and RFP-tubulin (red). Total time=5 min (10 sec/frame). Strain is FC2472.

Supplementary References

Basu, R., and Chang, F. (2011). Characterization of dip1p reveals a switch in Arp2/3-dependent actin assembly for fission yeast endocytosis. Curr Biol *21*, 905-916.

Marks, J., Hagan, I.M., and Hyams, J.S. (1986). Growth polarity and cytokinesis in fission yeast: the role of the cytoskeleton. J Cell Sci Suppl *5*, 229-241.

Sirotkin, V., Berro, J., Macmillan, K., Zhao, L., and Pollard, T.D. (2011). Quantitative analysis of the mechanism of endocytic actin patch assembly and disassembly in fission yeast. Mol Biol Cell *21*, 2894-2904.

Wu, J.Q., and Pollard, T.D. (2005). Counting cytokinesis proteins globally and locally in fission yeast. Science *310*, 310-314.